Age of Palos Verdes submarine debris avalanche, southern California

William R. Normark *, Mary McGann, Ray Sliter

Coastal and Marine Geology, US Geological Survey, Menlo Park, CA 94025 USA

Abstract

The Palos Verdes debris avalanche is the largest, by volume, late Quaternary mass-wasted deposit recognized from the inner California Borderland basins. Early workers speculated that the sediment failure giving rise to the deposit is young, taking place well after sea level reached its present position. A newly acquired, closely-spaced grid of high-resolution, deep-tow boomer profiles of the debris avalanche shows that the Palos Verdes debris avalanche fills a turbidite leveed channel that extends seaward from San Pedro Sea Valley, with the bulk of the avalanche deposit appearing to result from a single failure on the adjacent slope. Radiocarbon dates from piston-cored sediment samples acquired near the distal edge of the avalanche deposit indicate that the main failure took place about 7500 yr BP.
© 2003 Elsevier B.V. All rights reserved.

Keywords: submarine landslide; debris avalanche; California Borderland; turbidite fan valley; basin sedimentation

1. Introduction

Acquiring a history of submarine mass failure events, offshore of major coastal metropolitan areas, is necessary in assessing the potential for locally generated destructive tsunamis as a result of landsliding. Thus, the data used in this study were obtained as part of a project to identify and define earthquake and submarine landslide hazards in the area offshore of southern California. High-resolution multichannel and deep-towed boomer seismic-reflection profiles were acquired

during four marine surveys from 1998 to 2002 located between the US–Mexican border in the south to offshore Santa Barbara, California, in the north. Piston-core samples from the same area were acquired in 1998 and 1999. The data extend over most of the project area from near the coast to about 50 km offshore, and thus are restricted to the inner basins and shelf areas of the California Borderland. Submarine landslides and debris flows of Holocene age have been documented in all of the basins, especially in proximity to active faults near basin margins (Gorsline et al., 1984; Normark and Piper, 1998; Eichhubl et al., 2002; Hampton et al., 2002). Most of the mass-wasted deposits are relatively small, generally well less than 5 km in length (e.g. fig. 8 in Normark and Piper, 1998), but the large and blocky Palos Verdes debris avalanche is easily

---

* Corresponding author. Tel.: +1-650-329-5200;
Fax: +1-650-329-5198.
  E-mail addresses: wnormark@usgs.gov (W.R. Normark),
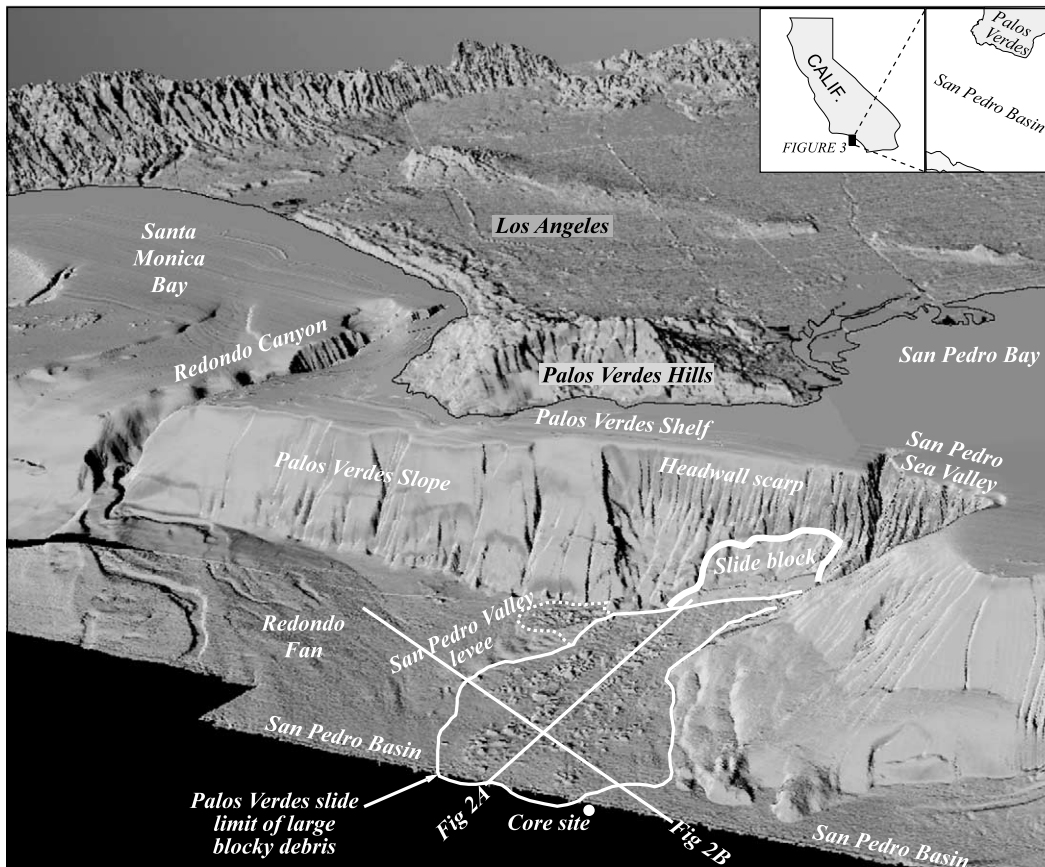mmcgann@usgs.gov (M. McGann), rsliter@usgs.gov
(R. Sliter).

Fig. 1. Multibeam shaded-relief oblique view looking northeast of the Palos Verdes submarine debris avalanche from Dartnell and Gardner (1999), as modified from Lee et al. (2002) and Hampton et al. (2002). Terminology used follows Hampton et al. (2002) and their area of flow deposit and runout blocks is identified as a debris avalanche following the definitions in Locat and Lee (2002) and Locat et al. (in press). Outline of Palos Verdes debris avalanche based on seismic-reflection (this study) and multi-beam data. Location of profiles in Fig. 2 and position of core site for both O2-99-SC, 510P1 and 510P2 (Fig. 8) is shown. Inset maps give location of study area.

the most prominent, extending out more than 10 km seaward from the base of the slope failure (Hampton et al., 2002) (Figs. 1 and 2). The debris avalanche covers slightly more than 50 km², and Hampton et al. (2002) show that it is associated with a slide block on the lower slope that is about 5 km wide.

The Palos Verdes debris avalanche was recognized from echograms obtained fifty years ago (Emery and Terry, 1956) as an area of hummocky and irregular topography. Gorsline et al. (1984), using seismic-reflection profiles, defined the area of the Palos Verdes 'slide' as a 'hummocky area [that] is a blocky slide and slump' (from the cap-

tion to their fig. 16). Gorsline et al. further suggested that the sediment failure resulted from 'metastability' caused by high sedimentation rates and that 'recent mass movement (c. 100 to 500 yrs old) has been observed in some of our recent profiles.' No direct dating of the failure was done.

Hampton et al. (1996) used 3.5-kHz seismic-reflection profile data to identify the main scarp of the Palos Verdes failure and recognized that the failure resulted in a large slide deposit on the lower slope as well as a flow deposit on the more gently sloping basin floor (fig. 11 in Hampton et al., 2002). Hampton et al. (2002), using multi-beam bathymetry and a closely spaced grid of
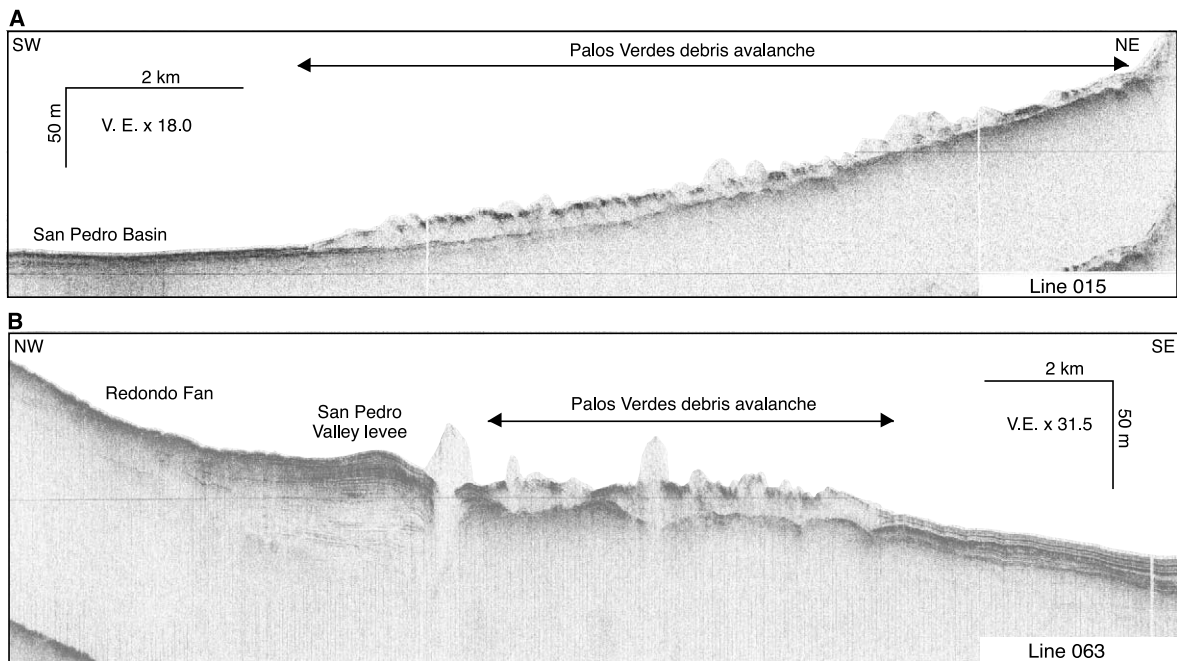
Fig. 2. Dip (line 015) and strike (line 063) deep-tow boomer seismic-reflection profiles across the Palos Verdes debris avalanche. Location of profiles shown in Figs. 1 and 3.

high-resolution seismic-reflection data and side-scan-sonar images, demonstrate the headwall scarp to be well defined and as shallow as 140 m water depth. Their multibeam bathymetry clearly images the slide mass at the base of the slope (Fig. 1).

The tsunami thought to have been created by the Palos Verdes debris avalanche has been evaluated by Locat et al. (2000), Bohannon and Gardner (2004) and Locat et al. (2004). Bohannon and Gardner (2004) suggest tsunami heights of about 10 m amplitude that might affect the local coastal areas. Locat et al. (2004) suggest amplitudes of 10–50 m and point out that a lack of knowledge about the initial conditions of the failure cause such a wide range in estimated amplitude of the tsunami. Further, the age of the failure has not been determined directly but is only guess estimated at ca. 100–500 yr BP (Gorsline et al., 1984). Therefore, it is the object of this study to accurately date the age of the deposit by using a combination of high-resolution seismic-reflection profiles and coring, thereby providing some idea of the frequency of events for hazard

assessment offshore Los Angeles. A critical factor is whether the deposit represents single or multiple failure events.

2. Methods

2.1. Seismic-reflection profiles

The high-resolution seismic-reflection profiles were acquired with a typical line spacing of 2–4 km. This allows the Palos Verdes debris avalanche to be mapped in detail. The debris avalanche deposit is not thick enough for its base to be clearly imaged on multichannel seismic-reflection profiles, but the base can be identified with Huntec deep-tow boomer profiles used in this paper (Figs. 3 and 4). The methodology used is as follows.

The Huntec Deep-Towed Seismic (DTS) boomer system was towed between 50 and 150 m below the sea surface (depending upon the water depth). Acoustic penetration of the boomer system is typically 0.1 s ($\sim$75 m subbottom) in basin turbidite and mass-wasted deposits, providing resolution of
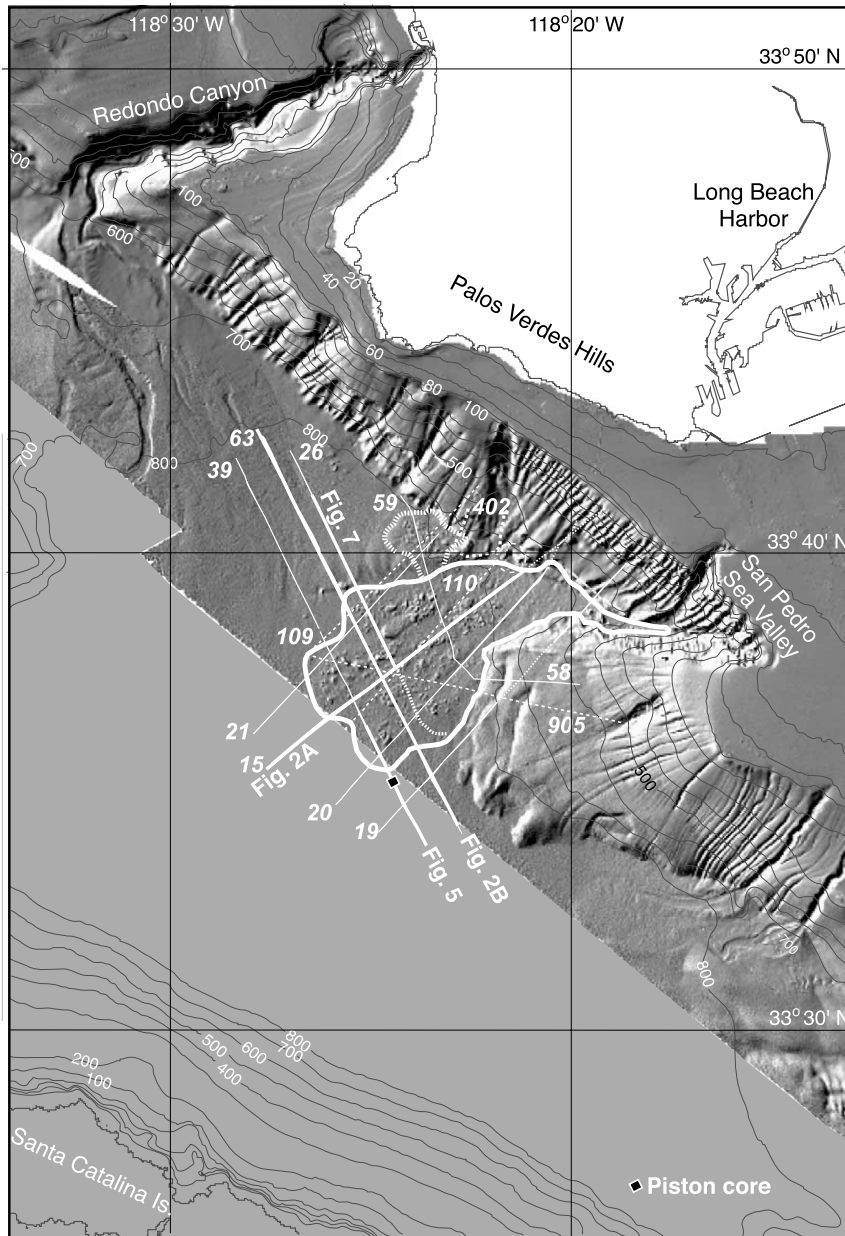
Fig. 3. Bathymetric map (NOAA, 1998) with shaded relief from multibeam bathymetry (Dartnell and Gardner, 1999) showing deep-tow Huntec boomer profiles used in this study and outline of the Palos Verdes debris avalanche. The view is vertical with illumination from the north; horizontal scale is given by the lines of latitude (10 min latitude is 18.5 km). Bathymetric contours in meters. Solid lines are from cruise A1-98-SC; dashed lines from cruise A1-00-SC. Heavy lines locate profiles illustrated in Figs. 2, 5 and 7.
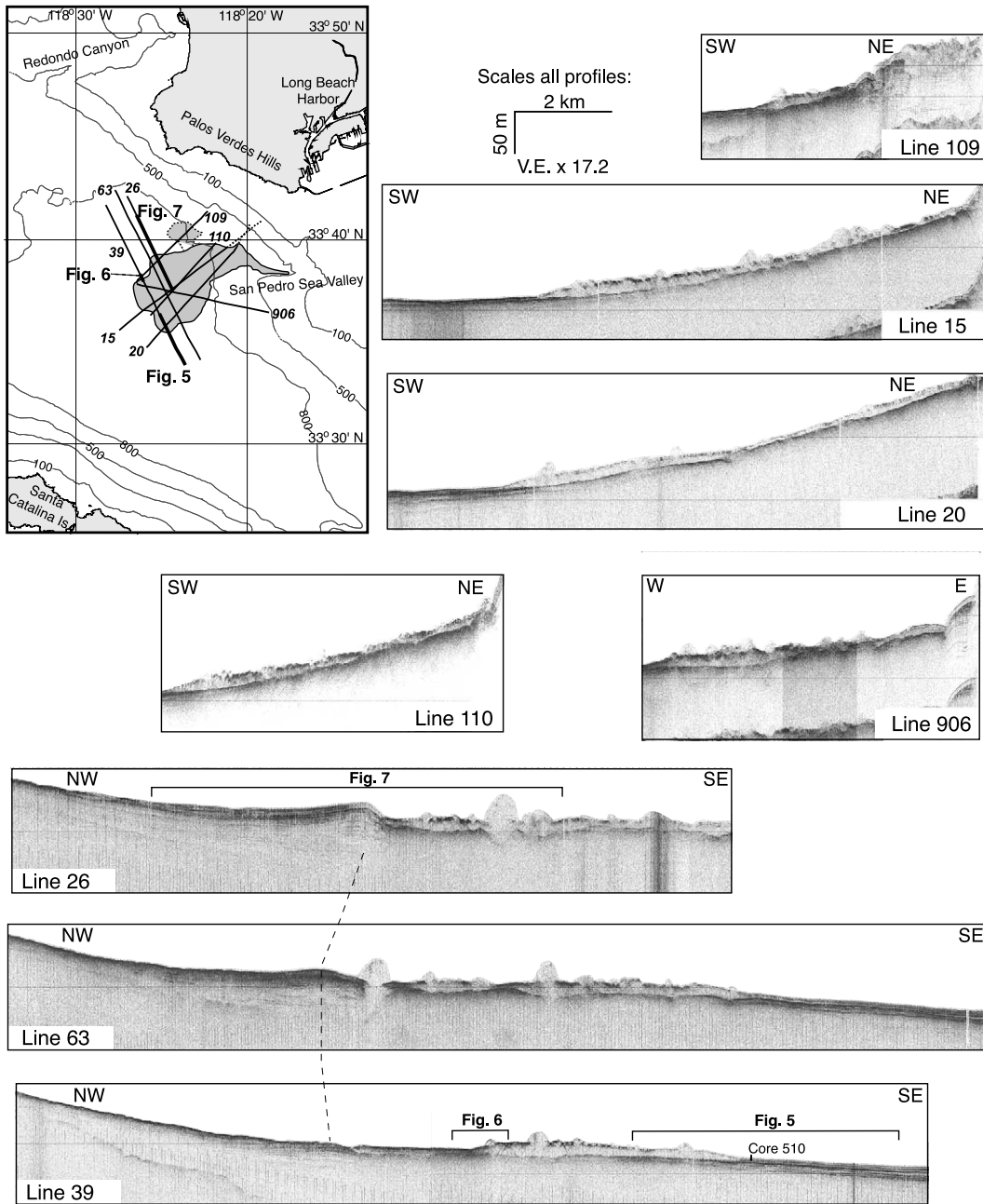
Fig. 4. Huntec boomer profiles across the Palos Verdes debris avalanche (gray shading) showing the blocky surface relief and the strong reflecting horizon that underlies the blocky debris on all profiles. This surface can be seen everywhere except under the thickest debris blocks. Inset gives location of the illustrated profiles. Bathymetric contour interval for location map is in meters.

better than 0.5 ms (0.4 m). Power output was 375 J, with a firing rate that was also dependent on water depth, ranging from 0.5 s over the upper basin slopes to 1.67 s over the deeper basin areas. Returning signals were received with a streamer towed from the deep-tow sled that housed the boomer acoustic source. The data were recorded without using bandpass filters or gain algorithms at a 0.25-s sweep in SEGY format on a magneto-optical disc (during the 1998 cruise) and on a Delph system harddisc (during 2000). The signals were then filtered at 640–4000 Hz. The average survey speed of about 4 kt (7.4 km/h) resulted in a shot spacing between 1.5 and 2.5 m for the deep-tow boomer profiles.

The Huntec system was generally used in deeper water (>300 m) to avoid interference from the transmitted acoustic pulse that is reflected from the sea surface. This operational limit to the effective use of the Huntec system, together with a regulatory limitation that prevented use of the multichannel seismic-reflection system within three miles of the coast, resulted in our data collection being primarily limited to the area of the debris avalanche. The hazard survey provided lit-

tle new information about the headwall scarp area, which lies above 300 m water depth and within three miles of the coast, and is discussed in Hampton et al. (2002).

2.2. Radiocarbon dating

The dip profiles in Figs. 2A and 4 show that the debris avalanche extends from the base of the slope and over-rides turbidites on the gently sloping floor of San Pedro Basin. The profile in Fig. 2B from near the southern margin of the avalanche deposit shows well-defined reflection horizons lateral to and continuous with (i.e. connected to) the edge of the debris avalanche that could be used to determine the age of the deposit. The age of the bedded sequences below and above the acoustically transparent layer that is continuous with the debris avalanche will bracket the time of the mass failure event.

The surface on which the deposit rests is within 4 m of the seafloor in some areas around the margins of the debris avalanche and could be accessed by a wire-line piston core (Figs. 2 and 4). To date the emplacement of the debris avalanche,

Table 1
Radiocarbon ages from piston cores O2-99-SC 510P1 and 510P2 near the southern margin of the Palos Verdes slide and calculated calendar ages

Hole-Core-Section, Interval (cm)	Material (foraminifera)	Depth[a]	Unit (Fig. 8)	^{14}C age (yr BP)	Corrected age (yr BP)[b]	Calendar age (yr BP)[c]
O2-99-SC 510P1		(mcd)				
sec. 1, 24–26 cm	N. pachyderma	0.25	5	2020 ± 30	1280 ± 30	2723 ± 65
sec. 1, 83–85 cm	Mixed planktic	0.84	4	4140 ± 35	3340 ± 35	3652 ± 90
sec. 1, 115–117 cm	N. pachyderma	1.16	3	5180 ± 45	4380 ± 45	5029 ± 180
sec. 1, 143–145 cm	N. pachyderma	1.44	3	6230 ± 45	5430 ± 45	6262 ± 70
sec. 2, 50–52 cm	N. pachyderma	2.01	2	8320 ± 40	7520 ± 40	8371 ± 60
sec. 2, 94–96 cm	N. pachyderma	2.45	2	8870 ± 55	8070 ± 55	8946 ± 235
sec. 3, 77–79 cm	N. pachyderm	3.78	1	9850 ± 55	9050 ± 55	10263 ± 425
O2-99-SC 510P2		(mbsf)				
sec. 1, 50–52 cm	N. pachyderma	0.51	5	2030 ± 40	1230 ± 40	2714 ± 85
sec. 2, 18–20 cm	N. pachyderma	1.69	3	4910 ± 80	4110 ± 80	4714 ± 190
sec. 2, 50–52 cm	N. pachyderma	2.01	3	6270 ± 45	5470 ± 45	6280 ± 95
sec. 2, 80–82 cm	N. pachyderma	2.31	3	6870 ± 45	6070 ± 45	6951 ± 120
sec. 3, 68–70 cm	N. pachyderma	3.69	1	9000 ± 50	8200 ± 50	9012 ± 410
sec. 3, 95–97 cm	N. pachyderma	3.96	1	9210 ± 70	8410 ± 70	9204 ± 140

[a] Sample depth in mbsf for core 510P2, which recovered the water/sediment interface. For core 510P1, which did not recover the water/sediment interface, depths are given in mcd, distance below top of core.

[b] Ages were calibrated using a reservoir age of 800 years following Southon et al. (1990) and Kienast and McKay (2001).

[c] Calendar ages were calculated using Radiocarbon Calibration Program Revision 4.3 (CALIB 4.3) from Quaternary Isotope Laboratory, University of Washington based on Stuiver and Reimer (1993).
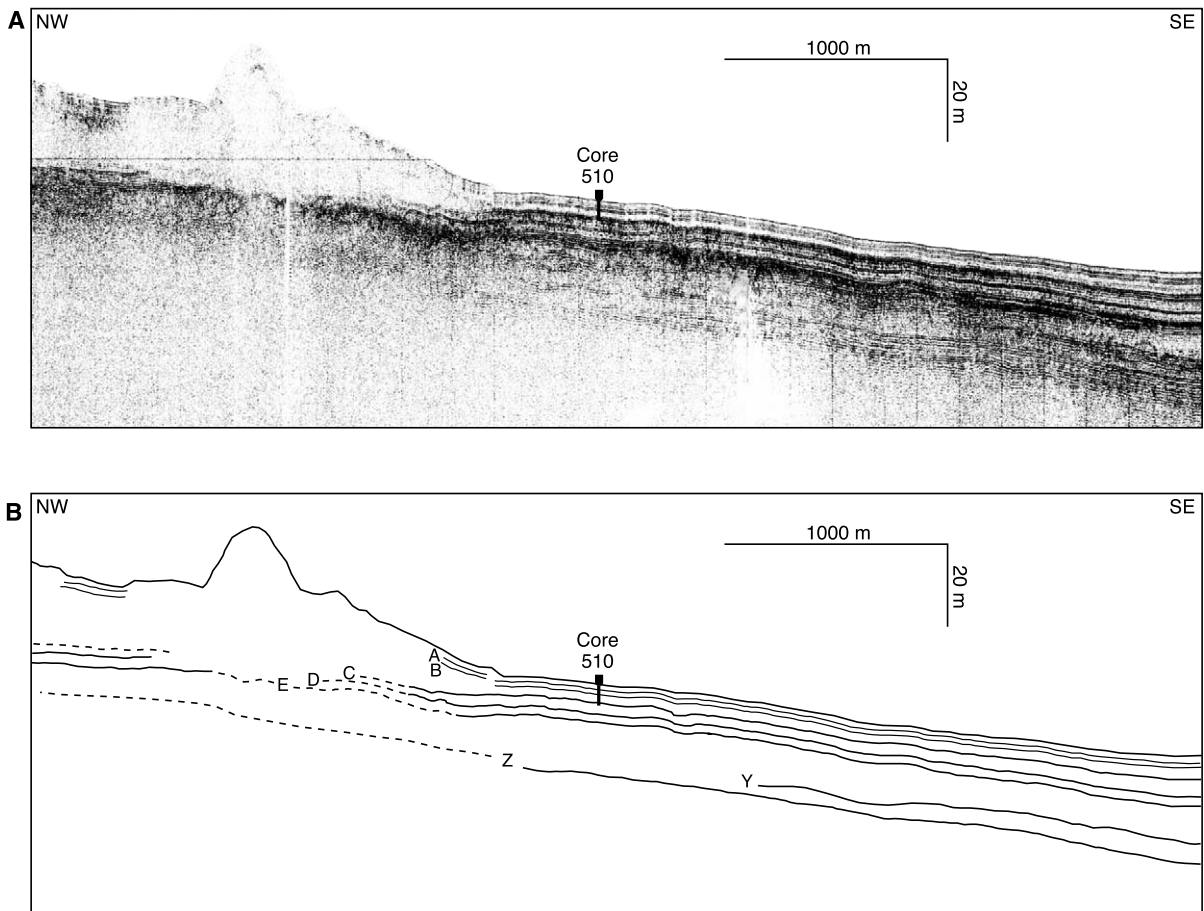
Fig. 5. (A) Deep-tow boomer seismic-reflection profile across the southern margin of the Palos Verdes debris avalanche and the position of cores O2-99-SC, 510P1 and 510P2. Profile location shown in Fig. 3. The core locations might be as much as 160 m apart based on position of the ship; the vertical scale of the core symbol is drawn to scale. (B) Line-drawing interpretation demonstrates that the upper part of the cored sequence, which includes the A and B reflectors, extends onto the surface of the debris avalanche. The cores penetrated a well-bedded sequence (the top of which is reflector C) that is overlain by the debris avalanche deposit at its margins but is eroded or deformed under the main body of the deposit. A high-amplitude reflection interval with an irregular surface (reflector E) can be traced under the avalanche deposit throughout the area (Fig. 4).

a piston core (510P1) was obtained on Huntec line 39 about 450 m from the southern edge of the deposit (Figs. 3 and 4). A second core (510P2), located less than 200 m away from the first, was also taken because 510P1 was shorter than expected and might not have reached the reflector seen to underlie the debris avalanche on all of the profiles (Fig. 4). Post-cruise, the cores were split and photographed in our onshore laboratory, and subsamples taken for radiocarbon-age dating. X-radiographs of non-bedded in-

tervals of the cores were taken to help determine the depositional processes involved.

Sediment ages for cores 510P1 and 510P2 were determined by accelerator mass spectrometry (AMS) ^{14}C, using planktic foraminifera. Twelve radiocarbon dates were determined using *Neogloboquadrina pachyderma*, and one additional sample used a mixed planktic foraminiferal assemblage (Table 1). The CALIB 4.3 program (Stuiver et al., 1998) was used to calculate calendar ages for these radiocarbon dates. A reservoir

age of 800 yr was chosen for these planktic fora-minifera (following Southon et al., 1990; Kienast and McKay, 2001), for radiocarbon ages younger than 12 000 years.

3. Results

3.1. Morphology and structure of the Palos Verdes debris avalanche

The debris avalanche runout extends more than 10 km from the base of the slope (Fig. 3). If measured along the axis of the San Pedro Sea Valley and its turbidite channel extension, the avalanche length is more than 14 km. The blocky nature of the deposit is well illustrated in all of the lines shown in Fig. 4, and 20-m relief of blocks in the debris is common. The strike profile of Fig. 2B (line 63) shows standing blocks with relief of about 40 m above the base of the deposit. In all dip profiles (Fig. 4), the margin of the flow forms a pronounced wedge.

During the emplacement of the debris ava-lanche, reflections from sediment layers that are presently as shallow as 4 m below the seafloor around the margin of the deposit were buried. Where the avalanche deposit is thicker, however, these reflections have been eroded or incorporated in the slide mass (Fig. 5). The margin of the de-bris deposit extends laterally through the core site as an acoustically transparent layer above the closely-spaced parallel reflectors that correspond to the deepest interval recovered at the core sta-tion (the core symbol in Fig. 5 is drawn to correct vertical scale). The base of the debris avalanche seen on all of the Huntec profiles (Fig. 4) is a high-amplitude reflection that is about 8 m below seafloor (mbsf) at the core site. High-amplitude reflections are typical of sandy deposits where sample control is available for the seismic-reflec-tion data in adjacent basin areas (see Piper et al., 1999).

The sediment interval overlying the avalanche deposit, which includes the two upper reflections ('A' and 'B' in the line-drawing interpretation in Fig. 5) observed on the Huntec profiles at the core site, is seen to onlap the wedge-shaped margin of
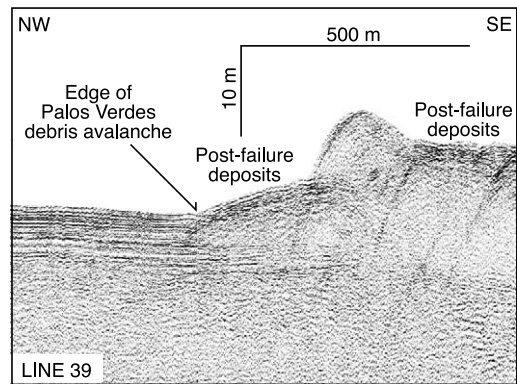

Fig. 6. Full-resolution display of a deep-tow boomer seismic-reflection profile across the northern margin of the Palos Verdes debris avalanche on the floor of the leveed valley extending from San Pedro Sea Valley (location in Fig. 4). Parallel-bedded reflectors (indicated as post-failure deposits) on the floor of the valley drape the margin of the debris ava-lanche and a similar acoustic sequence is seen on top of the lower-relief part of the avalanche debris to the southeast of a large block.

the avalanche deposit. Equivalent reflections are also seen on the northern edge of the avalanche and in areas where the gradient of the relief on the surface of the debris avalance is less steep (e.g. Figs. 6 and 7).

3.2. San Pedro Sea Valley levee

The headwall scarp of the Palos Verdes mass failure (slide and debris avalanche) extends for about 10 km along the slope that forms the right-hand wall (looking downstream) of the San Pedro Sea Valley (Fig. 3; Hampton et al., 2002). Before the debris avalanche was emplaced, San Pedro Sea Valley fed a small turbidite system on the floor of San Pedro Basin. A prominent levee extends west–southwest from the base of the slope for a distance of about 6 km (Fig. 1). The levee has distinct arcuate sediment waves typical of the righthand levees of many submarine fans in the Northern Hemisphere (Wynn and Stow, 2002; Normark et al., 2002). The levee relief in a basin-ward direction decreases abruptly between line 26 and line 63, and sediment from the Redondo Fan to the north onlaps the backside (north side) of the levee (Figs. 4 and 7). In our most seaward profile (line 39), which is less than 1.5 km from
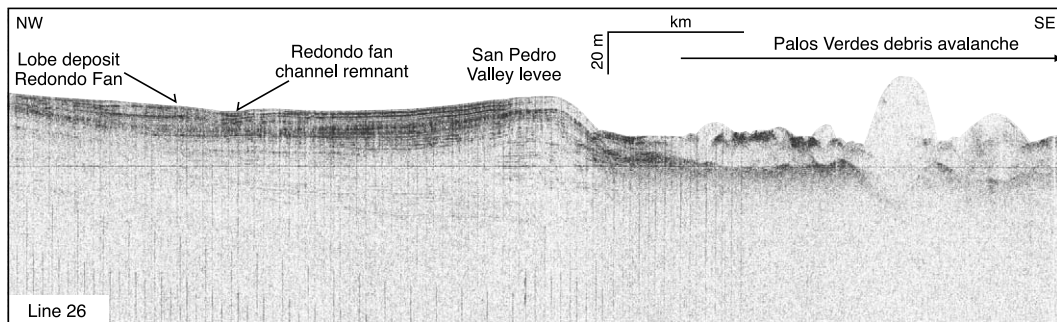
Fig. 7. Section of deep-tow boomer seismic-reflection profile of line 26 parallel to the basin margin across the Palos Verdes debris avalanche showing the confining effect of the turbidite channel levee extending from the north wall of the San Pedro Sea Valley. Profile location shown in Fig. 3. The youngest sediment on the levee crest appears continuous with the youngest sediment on Redondo Fan to the north.

line 63, the levee relief is almost non-existent at the seafloor and is nearly completely buried by sandy lobe and channel deposits from the Redondo Fan. The levee appears to have acted as a diversion dam that forces much of the Redondo Fan sediment to the southwest (Fig. 1).

The northern levee of San Pedro Sea Valley forms the northern boundary of the Palos Verdes debris avalanche from the base of the slope seaward for about 4 km. Farther west, the northern edge of the debris avalanche pinches out over what was the floor of the turbidite channel extending from the San Pedro Sea Valley. By line 39, the edge of the debris is about 2.5 km south of the inner wall of the levee (Fig. 4).

The southern boundary of the deposit is the south wall of San Pedro Sea Valley and its continuation southward along the base of the San Pedro Basin slope (Figs. 1 and 3). The debris avalanche deposit buries the floor of the fan valley from water depths as shallow as 550 m, which is near the break in slope of the valley axis, seaward to the flat-lying basin floor (Figs. 3 and 4). The western and southern limits of the debris avalanche appear as a sharp wedge-shaped toe on all profiles (Fig. 4).

3.3. Core descriptions and correlation

Fig. 8 shows the sediment logs from the two cores (510P1 and 510P2) obtained near the margin of the deposit, and bulk-density profiles are also shown to help correlate the cores. Five sedimentary units (Units 1–5 in Fig. 8) are represented. Unit 1, at the bottom of both cores, consists of a sequence of laminated silts and parallel-bedded silty sand and sand units. These turbidite deposits are overlain by a ±1-m-thick interval of muddy sediment with deformed silt beds and irregular blebs of silt (Unit 2). The term bleb refers to small patches of unconsolidated silt-sized sediment (therefore not a clast) seen at the split core surface that cannot be clearly explained by normal depositional processes, disrupted bedding, or section of a filled burrow, but more probably results from soft sediment deformation. The upper parts of the cores (Unit 3–5) contain only a few thin silt beds, in contrast to the sequences at the bottom of the cores. The contacts between the muddy debris flow unit and turbidite and muddy sequences below and above are not sharp; no clear contact is observed.

The sequence of turbidite beds at the bottom of the cores is more than 1 m shallower in core 510P1 than in 510P2. In both cores, the fine-grained turbidites of Unit 1 are overlain by a structureless mud (Unit 2) with a few inclusions of silt blebs and contorted, and apparently truncated, silt beds. X-radiographs of the split cores confirm the lack of internal bedding and apparent chaotic nature of Unit 2 in both cores. Unit 2 is interpreted as deposited from a muddy debris flow that has one or more episodes of deposition between 9000 and 7000 yr BP. Despite the proximity of the two cores, the debris flow unit is about 60 cm thinner in core 510P1. The debris flow sedi-
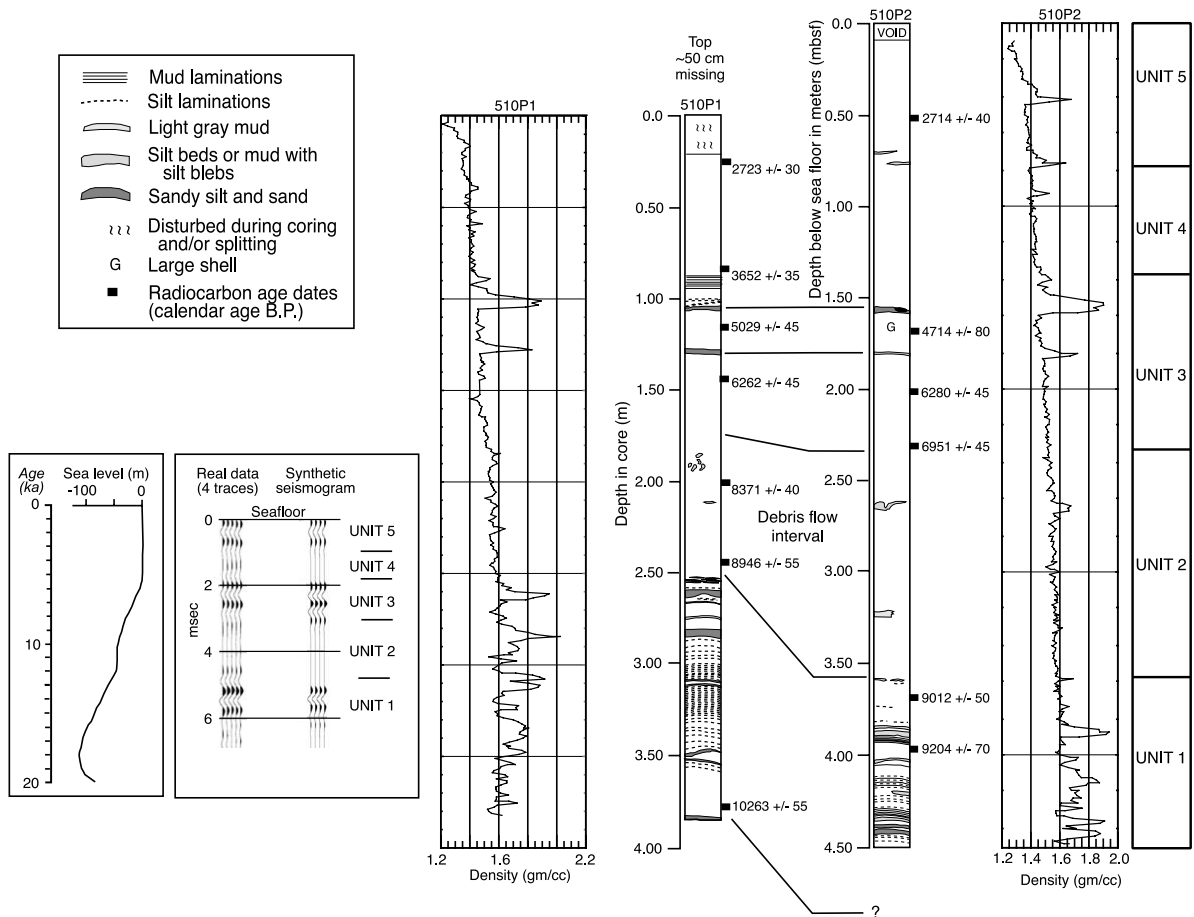
Fig. 8. Detailed sediment logs constructed from visual descriptions of piston cores O2-99-SC, 510P1 and 510P2 immediately south of the Palos Verdes debris-avalanche deposit (location of cores in Figs. 1, 3 and 5). The γ-ray density profiles for both cores are shown as well as the ¹⁴C dates (Table 1). The correlation between the closely spaced cores, which is based on sedimentology, density and velocity logs, and X-radiography, indicates that the upper half meter (approximately) of sediment at the location of core 510P1 was not recovered. The synthetic seismogram is based on core 510P2, which sampled the seafloor interface.

ment of Unit 2 is overlain by Unit 3, a thin (0.7–1 m) interval with two thin silty sand beds and laminated mud and silt intervals (core 510P1 only), indicating that more normal turbidite and hemipelagic mud deposition resumed after the debris flow was implaced. The sand beds have sharp bases and show normal grading locally. The density profiles associated with these bedded intervals are similar, primarily reflecting the two sandy horizons. The correlation shown in Fig. 8 is based on the match of these sandy beds and their associated log properties. The correlation suggests that core 510P1 did not recover the upper 0.5 m

(approximately) of sediment at the core site. The discontinuous silt lamina near 0.7 mbsf in 510P2 were not observed in 510P1, but the disturbance during core splitting may have obscured these thin units. Alternately, part of the upper section of both cores could be a younger muddy debris flow. The synthetic seismogram in Fig. 8 shows the reflections from the tops of Units 3 and 5 as observed in the deep-tow boomer records.

3.4. Age of sediment sequence

The radiocarbon ages based on planktic fora-

minifera (Fig. 8 and Table 1) provide additional data for the correlation of the cores based on visual description and X-radiographs. The top of the thin-bedded turbidite sequences in the lower parts (Unit 1) of both cores is about 9000 yr BP. The two deepest radiocarbon ages in each of the cores show that the sedimentation rate for this turbidite interval is more than 100 cm/10^3 yr (101 cm/10^3 yr in 510P1 between 2.45 m core depth (mcd) and 3.78 mcd), and 140 cm/10^3 yr in 510P2 between 3.69 and 3.96 mbsf (Table 1).

Sedimentation rates are much lower for the upper bedded interval (Unit 3; Fig. 8) being only about 25% of the rates for the thin bedded turbidites in Unit 1 at the base of both cores (23.0 cm/10^3 yr in 510P1 between 0.84 and 1.44 mcd, and 27.7 cm/10^3 yr in 510P2 between 1.69 and 2.31 mbsf; Table 1). The debris flow in cores 510P1 and 510P2 is roughly bracketed between the two bedded intervals, or between about 7000 and 9000 yr BP (Fig. 8). The one dated sample from the debris-flow interval at 2.01 mcd in 510P1 is 8371 yr BP in age, which only gives the age of some of the material incorporated in the flow. Because the deep-tow boomer profiles show that the debris avalanche might have incorporated sediment that is younger than the strongly reflective thin-bedded turbidite sequence recovered at the bottom of both cores, the age of the failure is probably closer to the younger 7000 yr BP limit.

4. Discussion

The Palos Verdes debris avalanche rests on turbidite fill of the San Pedro Sea Valley. The turbidite fill is generally flat-lying except for small-scale channel relief that might be the valley thalweg in the floor of the turbidite valley (see lines 39 and 63, Fig. 4). Generally, the base of the avalanche deposit is more irregular and might reflect relief of an earlier failure episode (see southeast end of line 26 and the central part of line 906 in Fig. 4). The high-resolution deep-tow boomer profiles do not show any prominent internal reflections within the debris avalanche that would suggest multiple failure events at least of the scale that delivered the

larger 20+ m high relief of blocks in the main deposit.

To estimate the younger limit for the age of the debris flow, the sedimentation rate of the upper bedded sequence was extrapolated downward from the closest age above the contact shown in Fig. 8 for each core. In 510P1, the top of the debris flow is estimated to be 7825 yr BP, whereas in 510P2 of the top is estimated at 7275 yr BP. It is reasonable, therefore, to place the time of failure at about 7500 yr BP.

The debris avalanche deposit, which is interpreted as one main failure event, occupies the time interval between 7500 yr BP and the top of Unit 1. Unit 2 in both cores has less sediment accumulated than would have accrued at the depositional rates observed for Unit 1. This abrupt change might reflect the fact that there was an early failure that blocked the floor of San Pedro Sea Valley and deflected turbidite sedimentation away from the area of core site 510. Alternatively, sediment supply to the San Pedro Sea Valley may have been reduced as a result of sea-level rise and/or tectonic activity on the Palos Verdes fault, which lies just east of the head of the valley. The wedge-shaped margin of the debris avalanche along its northern edge is onlapped by flat-lying reflectors, interpreted as turbidites from Huntec boomer records (line 39, Figs. 4 and 6). This onlapping sequence might have come from continued turbidity current activity in San Pedro Sea Valley after the debris avalanche. It is more likely, however, that some of the sediment burying the northern edge of the debris is from Redondo Fan (Fig. 7). In either case, there are no sediment core data to provide an independent estimate of the upper age limit for the debris avalanche based on more recent deposition on its northern margin.

The Huntec boomer records show that the margins of the debris avalanche are onlapped by sediment with a few reflectors subparallel with the seafloor but with low reflection amplitude compared to the turbidite sequences (Unit 1 and below; Figs. 5 and 6). As noted earlier, the upper part of the cores include thin muddy debris flows (Units 2 and 4) and thin-bedded turbidites (Unit 3). A comparison of sedimentation rates of Unit 3 with sediment at the top of the cores gives some

support to this idea. As noted earlier, the upper bedded interval Unit 3 in 510P1 has a sedimentation rate of 23.0 cm/10^3 yr; in 510P2, the rate is 27.7 cm/10^3 yr. The rate of accumulation for Units 4 and 5 above the upper bedded sequence in 510P1 is 36.7 cm/10^3 yr (assuming that 50 cm of sediment is missing from the top of the core) and the rate in 510P2 is 35.8 cm/10^3 yr. In both cores, the rate is significantly higher than that of the underlying Unit 3. The effects of sea-level rise tended to decrease continental margin sedimentation rates as sea level approached its current high stand; this relationship has been documented for many canyon-fed deep-water systems including the adjacent Santa Monica Basin (Piper et al., 1999). If some of the sediment in Unit 4 above the upper bedded sequence (Unit 3) is from a later mass failure event from the walls of San Pedro Sea Valley, it would explain the higher sedimentation rate. For example, the sedimentation rate for the structureless muddy section (Unit 4) above the upper bedded sequence is 63.5 cm/10^3 yr in 510P1 and 59.5 cm/10^3 yr in 510P2 (based on the two shallowest dates in each of the cores; Table 1). Descriptions of X-radiographs can be interpreted to suggest that about 40–50 cm of this muddy section might be the result of debris flow(s).

The deep-tow boomer data presented in this report support the argument that most of the blocky debris avalanche deposit resulted from one mass failure event, an interpretation that has been assumed in recent attempts to evaluate the tsunami run-up from the Palos Verdes mass failure (Locat et al., 2000, 2004; Bohannon and Gardner, 2004). Tsunami-generation models would benefit from an accurate estimate of the volume of material involved in the failure. A rough estimate of the volume of the deposit is ∼0.8 km^3 based on the deep-tow boomer data. As shown in Figs. 5 and 6, however, only the margins of the debris avalanche are resting on the ∼9000-yr-BP turbidite surface. Throughout most of the area of the debris avalanche, the base is an irregular surface cut into sandier turbidite deposits. It is difficult to estimate how much sediment from the basin floor and the floor of San Pedro turbidite valley might be incorporated into

the 7500-yr-BP avalanche deposit as imaged by the boomer profiles. Thus, the volume estimate of the avalanche deposit cannot be confidently related to the volume of sediment involved in the failure. Additionally, the volume of the associated debris flow deposit extending from the edge of the avalanche deposit cannot be determined with existing Huntec data, because these do not extend across the San Pedro Basin area (note the western limits of the dip lines in Fig. 3). The extent and volume of any turbidity-current deposits associated with the 7500-yr-BP failure also cannot be determined at this time. For estimating run-up amplitude of a tsunami caused by the Palos Verdes debris avalanche, a volume of 0.8 km^3 should be considered the maximum volume of failed sediment.

5. Conclusions

The Palos Verdes debris avalanche, which is the largest Holocene landslide in the inner continental Borderland, covers about 50 km^2 of the San Pedro Basin floor. Much of the debris is confined within the floor of a leveed fan valley extending from San Pedro Sea Valley. Radiocarbon dating of sediment from two piston cores near the edge of the debris avalanche show that emplacement occurred shortly before 7500 yr BP. New high-resolution deep-tow boomer seismic reflection profiles show little evidence to support multiple failures to generate the main body of the deposit.

cores. Reviews by M.A. Hampton, E. Geist, D.C. Mosher, and D.R. Tappin improved the manuscript.

References

Bohannon, R.G., Gardner, J.V., 2004. Submarine landslides of San Pedro Sea Valley, southwest Long Beach, California. Mar. Geol. 203, doi: 10.1016/S0025-3227(03)00309-8, this issue.

Dartnell, P., Gardner, J.V., 1999. Sea-floor images and data from multibeam surveys in San Francisco Bay, southern California, Hawaii, the Gulf of Mexico, and Lake Tahoe, California–Nevada. US Geological Survey Digital data Series DDS-55, version 1.0 (CD-ROM).

Eichhubl, P., Greene, H.G., Maher, N., 2002. Physiography of an active transpressive margin basin; high-resolution bathymetry of the Santa Barbara Basin, southern California continental borderland. Mar. Geol. 184, 95–120.

Emery, K.O., Terry, R.D., 1956. A submarine slope off southern California. J. Geol. 64, 271–280.

Gorsline, D.S., Kolpack, R.L., Karl, H.A., Drake, D.E., Fleischer, P., Thornton, S.E., Schwalbach, J.E., Savrda, C.E., 1984. Studies of fine-grained sediment transport processes and products in the California continental borderland. In: Stow, D.A.V., Piper, D.J.W. (Eds.), Fine-grained Sediments: Deep Water Processes and Facies. Blackwell Scientific Publishers, Oxford, pp. 395–415.

Hampton, M.A., Karl, H.A., Murray, C.J., 2002. Acoustic profiles and images of the Palos Verdes margin: Implications concerning deposition from the White's Point outfall. Cont. Shelf Res. 22, 841–857.

Hampton, M.A., Lee, H.J., Locat, J., 1996. Submarine landslides. Rev. Geophys. 34, 33–59.

Kienast, S.S., McKay, J.L., 2001. Sea surface temperatures in the subarctic northeast Pacific reflect millennial-scale climate oscillations during the last 16 kyrs. Geophys. Res. Lett. 28, 1563–1566.

Lee, H.J., Sherwood, C.R., Drake, D.E., Edwards, B.D., Wong, F., Hamer, M., 2002. Spatial and temporal distribution of contaminated, effluent-affected sediment on the Palos Verdes margin, southern California. Cont. Shelf Res. 22, 859–880.

Locat, J., Lee, H.J., 2002. Submarine landslides: Advances and challenges. Can. Geotech. J. 39, 193–212.

Locat, J., Lee, H.J., Locat, P., 2000. Mobility of the Palos Verdes debris avalanche, California, and potential tsunami generation. Eos, Trans. Am. Geophys. Union 81, F750.

Locat, J., Locat, P., Lee, H.J., Imran, J., 2004. Numerical analysis of the mobility of the Palos Verdes debris avalanche, California, and its implication for the generation of tsunamis. Mar. Geol. 20-3, doi: 10.1016/S0025-3227(03)00310-4, this issue.

NOAA, 1998, NOS Hydrographic Survey Data, US Coastal Waters. World Data Center for Marine Geology and Geophysics, Boulder, CO, Data Announcement 01-MGG-03 (data available at: http://www.ngdc.noaa.gov/mgg/fliers/01mgg03.html).

Normark, W.R., Piper, D.J.W., 1998. Preliminary evaluation of recent movement on structures within the Santa Monica Basin, offshore southern California. US Geological Survey Open-File Report 98-518, 60 pp.

Normark, W.R., Piper, D.J.W., Posamentier, H., Pirmez, C., Migeon, S., 2002. Variability in form and growth of sediment waves on turbidite channel levees. Mar. Geol. 192, 23–58.

Piper, D.J.W., Hiscott, R.N., Normark, W.R., 1999. Outcrop-scale acoustic facies analysis and latest Quaternary development of Hueneme and Dume submarine fans, offshore California. Sedimentology 46, 47–78.

Southon, J.R., Nelson, D.E., Vogel, J.S., 1990. A record of past ocean-atmosphere radiocarbon difference from the Northeast Pacific. Paleoceanography 5, 197–206.

Stuiver, M., Reimer, P.J., 1993. Extended ^{14}C database and revised CALIB radiocarbon calibration program. Radiocarbon 35, 215–230.

Stuiver, M., Reimer, P.J., Bard, E., Beck, J.W., Burr, G.S., Hughen, K.A., Kromer, B., McCormac, F.G., Plicht, J. van der, Spurk, M., 1998. INTCAL98 radiocarbon age calibration 24,000–0 cal BP. Radiocarbon 40, 1041–1083.

Wynn, R.B., Stow, D.A.V., 2002. Classification and characterization of deep-water sediment waves. Mar. Geol. 192, 7–22.